Electronic supplementary information

Bifunctional $Zn^{II}Ln^{III}$ dinuclear complexes combining field induced SMM behaviour and luminescence: Enhanced NIR lanthanide emission by 9-anthracene carboxylate bridging ligands.

María A. Palacios, Silvia Titos-Padilla, José Ruiz, Juan Manuel Herrera, Simon J. A. Pope, Euan K. Brechin, and Enrique Colacio

Table S1.- Elemental analyses for complexes **1-13**

Compound	Formula	Mw	% Cteor	(% Cexp)	% Hteor	(% Hexp)	% Nteor	(% Nexp)
1	C_{27} H_{40} N_5 O_{12} Zn Tb	850.93	38.11	(38.04)	4.74	(4.65)	8.23	(8.30)
2	C_{27} H_{40} N_5 O_{12} Zn Dy	854.51	37.95	(37,90)	4.72	(4.67)	8.20	(8.37)
3	C_{27} H_{40} N_5 O_{12} Zn Er	859.27	37.74	(37.70)	4.69	(4.61)	8.15	(8.24)
4	C_{27} H_{40} N_5 O_{12} Zn Yb	865.05	37.49	(37.55)	4,66	(4.73)	8.10	(8.20)
5	C_{25} H_{37} N_6 O_{13} Zn Er	862.24	34.82	(34.90)	4.33	(4.41)	9.75	(9.90)
6	C_{27} H_{47} N_6 O_{16} Zn Nd	921.32	35.20	(35.31)	5.14	(5.30)	9.12	(9.01)
7	C_{44} H_{52} N_7 O_{12} Zn Tb	1095.22	48.25	(48.40)	4.78	(4.91)	8.95	(9.07)
8	C_{44} H_{52} N_7 O_{12} Zn Dy	1098.80	48.10	(48.15)	4.77	(4.83)	8.92	(9.00)
9	C_{44} H_{52} N_7 O_{12} Zn Er	1103.56	47.89	(47.80)	4.75	(4.76)	8.88	(8.98)
10	C_{44} H_{52} N_7 O_{12} Zn Yb	1109.34	47.64	(47.53)	4.73	(4.75)	8.84	(8.80)
11	C_{61} H_{64} N_7 O_{11} Zn Yb	1309.60	55.94	(55.90)	4.93	(5.00)	7.49	(7.44)
12	C_{59} H_{67} N_6 O_{14} Zn Nd	1293.83	54.77	(54.86)	5.22	(5.30)	6.50	(6.60)
13	C_{44} H_{62} N_4 O_{17} Cl Zn Nd	1164.07	45.40	(45.48)	5.37	(5.45)	4.81	(4.90)

Table S2.- Crystallographic data for compounds **1-13**

Compound	**1**	**3**	**4**	**5**	**6**	**7**
Formula	$C_{27}H_{40}N_5O_{12}ZnTb$	$C_{27}H_{40}N_5O_{12}ZnEr$	$C_{27}H_{40}N_5O_{12}ZnYb$	$C_{25}H_{37}N_6O_{13}ZnEr$	$C_{27}H_{47}N_6O_{16}ZnNd$	$C_{44}H_{52}N_7O_{12}ZnTb$
M_r	850.93	859.27	865.05	862.24	921.32	1095.22
Crystal system	Triclinic	Monoclinic	Monoclinic	Orthorhombic	Monoclinic	Monoclinic
Space group (no.)	*P-1* (2)	*P21/n* (14)	*P21/n* (14)	*P212121* (19)	*P21/c* (14)	*P21/n* (14)
a (Å)	11.45081(14)	11.345(5)	11.3197(7)	10.7276(5)	10.686(5)	13.546(5)
b (Å)	14.77726(18)	14.542(5)	14.5238(9)	15.8243(7)	17.785(5)	23.332(5)
c (Å)	19.3346(2)	20.078(5)	20.1539(12)	17.8958(8)	20.049(5)	14.885(5)
a (°)	92.6221(10)	90.000(5)	90.00	90.00	90.000(5)	90.000(5)
β (°)	98.4836(10)	101.407(5)	101.7910(10)	90.00	102.148(5)	102.616(5)
γ (°)	90.9880(10)	90.000(5)	90.00	90.00	90.000(5)	90.000(5)
V (Å^3)	3231.50(7)	3247(2)	3243.5(3)	3037.9(2)	3725(2)	4591(2)
Z	4	4	4	4	4	4
D_c (g cm^{-3})	1.749	1.758	1.771	1.885	1.639	1.585
μ(Mo$K\alpha$) (mm^{-1})	2.981	3.373	3.673	3.609	2.098	2.119
T (K)	100(2)	100(2)	100(2)	100(2)	100(2)	100(2)
Observed reflections	16275 (13145)	5689 (5178)	5711 (5254)	5346 (5086)	6560 (5982)	8069 (7233)
R_{int}	0.0403	0.0323	0.0256	0.0302	0.0351	0.0268
Parameters	844	423	423	422	471	595
GOF	0.979	1.055	1.057	0.823	1.109	1.063
R_1[a, b]	0.0363 (0.0260)	0.0310 (0.0281)	0.0269 (0.0240)	0.0272 (0.0253)	0.0388 (0.0347)	0.0330 (0.0289)
wR_2[c]	0.0566 (0.0549)	0.0700 (0.0683)	0.0576 (0.0557)	0.0627 (0.0609)	0.0880 (0.0849)	0.0710 (0.0688)
Largest difference in peak and hole (e Å^{-3})	1.354 and -0.875	2.947 and -1.033	1.394 and -0.522	1.318 and -0.422	1.453 and -0.767	1.198 and -0.328

[a] $R_1 = \Sigma||F_o| - |F_c||/\Sigma|F_o|$.
[b] Values in parentheses for reflections with $I > 2\sigma(I)$.

[c] $wR_2 = \{\Sigma[w(F_o^2 - F_c^2)^2] / \Sigma[w(F_o^2)^2]\}^{1/2}$

Compound	**8**	**9**	**10**	**11**	**12**	**13**
Formula	$C_{44}H_{52}N_7O_{12}ZnDy$	$C_{44}H_{52}N_7O_{12}ZnEr$	$C_{44}H_{52}N_7O_{12}ZnYb$	$C_{61}H_{64}N_7O_{11}ZnYb$	$C_{59}H_{67}N_6O_{14}ZnNd$	$C_{44}H_{62}N_4O_{17}ClZnNd$
M_r	1098.80	1103.56	1109.34	1309.60	1293.83	1164.07
Crystal system	Monoclinic	Monoclinic	Monoclinic	Orthorhombic	Orthorhombic	Triclinic
Space group (no.)	*P21/n* (14)	*P21/n* (14)	*P21/n* (14)	*Pca21* (29)	*Pca21* (29)	*P-1* (2)
a (Å)	13.547(5)	13.533(5)	13.542(5)	22.4764(12)	22.664(5)	12.051(5)
b (Å)	23.341(5)	23.340(5)	23.319(5)	12.8315(7)	12.828(5)	12.325(5)
c (Å)	14.882(5)	14.868(5)	14.857(5)	19.7813(10)	19.893(5)	17.328(5)
α (°)	90.000(5)	90.000(5)	90.000(5)	90.00	90.000(5)	74.587(5)
β (°)	102.621(5)	102.600(5)	102.575(5)	90.00	90.000(5)	86.073(5)
γ (°)	90.000(5)	90.000(5)	90.000(5)	90.00	90.000(5)	83.022(5)
V (Å^3)	4592(2)	4583(2)	4579(2)	5705.0(5)	5784(3)	2461.0(16)
Z	4	4	4	4	4	2
D_c (g cm^{-3})	1.589	1.599	1.609	1.525	1.479	1.437
μ(MoK$_\alpha$) (mm^{-1})	2.206	2.411	2.623	2.117	1.373	1.593
T (K)	100(2)	100(2)	100(2)	100(2)	100(2)	100(2)
Observed reflections	8081 (7400)	8064 (7374)	8003 (7326)	8019 (7335)	9088 (8234)	8641 (6872)
R_{int}	0.0333	0.0399	0.0300	0.0711	0.0613	0.0559
Parameters	595	595	595	740	749	589
GOF	1.066	1.076	1.040	1.037	1.041	1.001
R_1[a, b]	0.0280 (0.0251)	0.0293 (0.0262)	0.0309 (0.0277)	0.0370 (0.0319)	0.0467 (0.0409)	0.0566 (0.0442)
wR_2[c]	0.0618 (0.0601)	0.0650 (0.0634)	0.0675 (0.0658)	0.0723 (0.0693)	0.0965 (0.0914)	0.0989 (0.0935)
Largest difference in peak and hole (e Å^{-3})	1.122 and -0.387	1.387 and -0.391	1.422 and -0.561	1.361 and -0.455	1.700 and -0.536	1.238 and -0.451

[a] $R_1 = \Sigma||F_o| - |F_c||/\Sigma|F_o|$.
[b] Values in parentheses for reflections with $I > 2\sigma(I)$.

[c] $wR_2 = \{\Sigma[w(F_o^2 - F_c^2)^2] / \Sigma[w(F_o^2)^2]\}^{½}$

Table S3.- Selected bond lengths and angles for complexes **1**-**13**

Compound	**1**	**1**	**3**	**4**	**5**	**6**
Ln(1)-Zn(1)	3.4662(3)	3.4570(3)	3.434(1)	3.4137(4)	3.4538(5)	3.637(1)
Ln(1)-O(2A)	2.460(2)	2.479(2)	2.386(3)	2.369(2)	2.416(3)	2.660(3)
Ln(1)-O(5A)	2.329(2)	2.280(2)	2.298(2)	2.280(2)	2.250(3)	2.338(3)
Ln(1)-O(25A)	2.231(2)	2.240(2)	2.209(2)	2.189(2)	2.195(3)	2.371(2)
Ln(1)-O(27A)	2.675(1)	2.726(2)	2.721(3)	2.777(2)	2.562(3)	2.654(3)
Ln(1)-O(2)bridge	2.313(2)	2.307(2)	2.295(3)	2.268(2)	2.422(3)	
Ln(1)-O(1B)nitrate			2.443(3)	2.423(2)	2.412(3	2.537(4)
Ln(1)-O(2B)nitrate			2.433(2)	2.408(2)	2.435(3)	2.554(3)
Ln(1)-O(1C)nitrate	2.492(2)	2.502(2)	2.435(3)	2.408(2)	2.439(3)	2.578(3)
Ln(1)-O(2C)nitrate	2.447(2)	2.483(2)	2.447(3)	2.428(2)	2.449(3)	2.578(3)
Ln(1)-O(1D)nitrate	2.471(2)	2.455(2)				2.577(3)
Ln(1)-O(2D)nitrate	2.494(2)	2.478(2)				2.559(1)
Zn(1)-N(12A)	2.180(2)	2.164(2)	2.256(3)	2.262(2)	2.170(4)	2.164(4)
Zn(1)-N(16A)	2.223(2)	2.240(2)	2.195(4)	2,194(3)	2.182(4)	2.186(4)
Zn(1)-N(20A)	2.226(2)	2.233(2)	2.256(3)	2.250(3)	2.251(4)	2.216(4)
Zn(1)-O(5A)	2.189(2)	2.172(2)	2.184(2)	2.177(2)	2.161(3)	2.117(2)
Zn(1)-O(25A)	2.071(2)	2.063(2)	2.097(2)	2.106(2)	2.045(3)	2.077(3)
Zn(1)-O(1)bridge	2.075(2)	2.057(1)	2.037(3)	2.041(2)	2.156(3)	
Zn(1)-O(1W)						2.219(3)
Ln(1)-O(5A)-Zn(1)	100.16(6)	101.86(6)	100.00(9)	99.96(9)	103.0(1)	109.4(1)
Ln(1)-O(25A)-Zn(1)	107.30(7)	106.87(7)	105.7(1)	105.26(9)	109.1(1)	109.5(1)
O(5A)-Ln(1)-O(25A)	70.07(6)	69.90(6)	72.02(8)	72.51(8)	70.4(1)	65.87(8)
O(5A)-Ln(1)-O(2)bridge	78.43(6)	78.82(6)	78.88(9)	79.80(8)	75.7(1)	
O(25A)-Ln(1)-O(2)bridge	80.88(6)	79.93(6)	80.86(9)	81.60(8)	78.9(1)	
O(5A)-Zn(1)-O(25A)	75.83(6)	75.32(6)	76.48(9)	76.23(8)	75.0(1)	75.2(1)
O(5A)-Zn(1)-O(1)bridge	93.36(6)	91.15(6)	90.35(9)	90.10(9)	87.3(1)	
O(25A)-Zn(1)-O(1)bridge	93.85(6)	95.28(6)	95.76(9)	95.48(9)	90.6(1)	
O(5A)-Zn(1)-O(1W)						84.1(1)
O(25A)-Zn(1)-O(1W)						85.5(1)

Compound	**7**	**8**	**9**	**10**	**11**	**12**	**13**
Ln(1)-Zn(1)	3.4646(7)	3.4550(7)	3.4346(7)	3.4160(7)	3.4213(8)	3.529(1)	3.556(1)
Ln(1)-O(2A)	2.465(2)	2.453(2)	2.431(2)	2.416(2)	2.408(4)	2.530(4)	2.527(3)
Ln(1)-O(5A)	2.289(2)	2.277(2)	2.259(2)	2.236(2)	2.254(4)	2.379(4)	2.397(2)
Ln(1)-O(25A)	2.230(2)	2.222(2)	2.201(2)	2.181(2)	2.205(4)	2.318(3)	2.298(3)
Ln(1)-O(27A)	2.606(2)	2.598(2)	2.599(2)	2.610(2)	2.854(4)	2.738(4)	2.686(2)
Ln(1)-O(17D)bridge	2.345(2)	2.340(2)	2.311(2)	2.299(2)	2.274(3)	2.412(4)	2.420(3)
Ln(1)-O(1B)nitrate	2.508(2)	2.482(2)	2.485(2)	2.378(2)	2.456(4)	2.586(4)	2.589(4)
Ln(1)-O(2B)nitrate	2.449(2)	2.443(2)	2.406(2)	2.475(2)	2.403(4)	2.549(4)	2.573(3)
Ln(1)-O(1C)nitrate[a]	2.448(2)	2.438(2)	2.422(2)	2.389(2)	2.382(4)	2.494(4)	2.499(4)
Ln(1)-O(2C)nitrate[b]	2.498(2)	2.495(2)	2.458(2)	2.443(2)	2.342(4)	2.473(4)	2.495(4)

Zn(1)-N(12A)	2.173(3)	2.175(2)	2.177(2)	2.179(3)	2.186(4)	2.196(4)	2.179(3)
Zn(1)-N16A)	2.222(3)	2.225(2)	2.224(2)	2.226(3)	2.200(5)	2.222(4)	2.226(4)
Zn(1)-N(20A)	2.283(2)	2.284(2)	2.279(2)	2.275(2)	2.244(5)	2.276(4)	2.258(4)
Zn(1)-O(5A)	2.186(2)	2.187(2)	2.179(2)	2.177(2)	2.146(4)	2.183(4)	2.185(3)
Zn(1)-O(25A)	2.057(2)	2.055(2)	2.055(2)	2.056(2)	2.115(4)	2.090(4)	2.073(2)
Zn(1)-O(16D)bridge	2.099(2)	2.099(2)	2.102(2)	2.102(2)	2.074(4)	2.061(4)	2.069(3)
Ln(1)-O(5A)-Zn(1)	101.43(8)	101.38(7)	101.40(7)	101.43(8)	102.1(2)	101.2(1)	101.7(1)
Ln(1)-O(25A)-Zn(1)	107.76(9)	107.72(8)	107.59(8)	107.45(9)	104.7(2)	106.3(2)	108.7(1)
O(5A)-Ln(1)-O(25A)	70.48(7)	70.69(6)	71.08(7)	71.51(7)	71.7(1)	69.7(1)	67.99(9)
O(5A)-Ln(1)-O(17D)bridge	77.76(7)	78.11(6)	78.46(7)	78.96(7)	78.9(1)	76.1(1)	77.12(9)
O(25A)-Ln(1)-O(17D)bridge	79.84(7)	80.05(6)	80.37(7)	80.63(7)	83.0(1)	78.6(1)	79.47(9)
O(5A)-Zn(1)-O(25A)	75.78(8)	75.64(7)	75.45(7)	75.09(8)	75.6(1)	77.8(1)	76.1(1)
O(5A)-Zn(1)-O(16D)bridge	91.04(7)	90.97(7)	90.83(7)	90.96(8)	91.8(1)	92.1(1)	90.4(1)
O(25A)-Zn(1)-O(16D)bridge	92.48(8)	92.40(7)	92.09(7)	92.01(8)	93.4(1)	93.8(1)	93.4(1)

[a] **11 y 12**, O(16C) anthracene. **13,** O(1M) methanol

[b] **11 y 12**, O(17C) anthracene. **13,** O(2M) methanol

Table S4.-Continuous Shape Measures calculation for **2**

```
MFF-9          13 Cs    Muffin
HH-9           12 C2v   Hula-hoop
JTDIC-9        11 C3v   Tridiminished icosahedron J63
TCTPR-9        10 D3h   Spherical tricapped trigonal prism
JTCTPR-9        9 D3h   Tricapped trigonal prism J51
CSAPR-9         8 C4v   Spherical capped square antiprism
JCSAPR-9        7 C4v   Capped square antiprism J10
CCU-9           6 C4v   Spherical-relaxed capped cube
JCCU-9          5 C4v   Capped cube J8
JTC-9           4 C3v   Johnson triangular cupola J3
HBPY-9          3 D7h   Heptagonal bipyramid
OPY-9           2 C8v   Octagonal pyramid
EP-9            1 D9h   Enneagon

Structure [ML9 ]        MFF-9         HH-9      JTDIC-9
TCTPR-9     JTCTPR-9      CSAPR-9     JCSAPR-9        CCU-9
JCCU-9        JTC-9       HBPY-9        OPY-9         EP-9 ,
2.274,      10.337,      11.809,       2.799,       4.168,
2.365,       3.521,       7.589,       8.958,      15.920,
14.999,      23.362,      36.124
```

Table S5.-Continuous Shape Measures calculation for **8**

```
MFF-9          13 Cs    Muffin
HH-9           12 C2v   Hula-hoop
JTDIC-9        11 C3v   Tridiminished icosahedron J63
TCTPR-9        10 D3h   Spherical tricapped trigonal prism
JTCTPR-9        9 D3h   Tricapped trigonal prism J51
```

CSAPR-9	8	C4v	Spherical capped square antiprism
JCSAPR-9	7	C4v	Capped square antiprism J10
CCU-9	6	C4v	Spherical-relaxed capped cube
JCCU-9	5	C4v	Capped cube J8
JTC-9	4	C3v	Johnson triangular cupola J3
HBPY-9	3	D7h	Heptagonal bipyramid
OPY-9	2	C8v	Octagonal pyramid
EP-9	1	D9h	Enneagon

Structure [ML9]	MFF-9	HH-9	JTDIC-9
TCTPR-9	JTCTPR-9	CSAPR-9	JCSAPR-9	CCU-9
JCCU-9	JTC-9	HBPY-9	OPY-9	EP-9
1.668,	9.091,	11.107,	2.761,	4.689,
2.000,	2.947,	8.196,	9.510,	15.240,
16.549,	22.853,	35.937		

Table S6.-Continuous Shape Measures calculation for **3**

MFF-9	13	Cs	Muffin
HH-9	12	C2v	Hula-hoop
JTDIC-9	11	C3v	Tridiminished icosahedron J63
TCTPR-9	10	D3h	Spherical tricapped trigonal prism
JTCTPR-9	9	D3h	Tricapped trigonal prism J51
CSAPR-9	8	C4v	Spherical capped square antiprism
JCSAPR-9	7	C4v	Capped square antiprism J10
CCU-9	6	C4v	Spherical-relaxed capped cube
JCCU-9	5	C4v	Capped cube J8
JTC-9	4	C3v	Johnson triangular cupola J3
HBPY-9	3	D7h	Heptagonal bipyramid
OPY-9	2	C8v	Octagonal pyramid
EP-9	1	D9h	Enneagon

Structure [ML9]	MFF-9	HH-9	JTDIC-9
TCTPR-9	JTCTPR-9	CSAPR-9	JCSAPR-9	CCU-9
JCCU-9	JTC-9	HBPY-9	OPY-9	EP-9
,2.342,	8.670,	11.539,	2.664,	3.667,
2.413,	3.606,	7.053,	8.316,	15.663,
15.296,	23.442,	35.508		

Table S7.- Continuous Shape Measures calculation for **5.**

MFF-9	13	Cs	Muffin
HH-9	12	C2v	Hula-hoop
JTDIC-9	11	C3v	Tridiminished icosahedron J63
TCTPR-9	10	D3h	Spherical tricapped trigonal prism
JTCTPR-9	9	D3h	Tricapped trigonal prism J51
CSAPR-9	8	C4v	Spherical capped square antiprism
JCSAPR-9	7	C4v	Capped square antiprism J10
CCU-9	6	C4v	Spherical-relaxed capped cube
JCCU-9	5	C4v	Capped cube J8
JTC-9	4	C3v	Johnson triangular cupola J3
HBPY-9	3	D7h	Heptagonal bipyramid
OPY-9	2	C8v	Octagonal pyramid
EP-9	1	D9h	Enneagon

Structure	[ML9]	MFF-9	HH-9	JTDIC-9
TCTPR-9	JTCTPR-9	CSAPR-9	JCSAPR-9	CCU-9
JCCU-9	JTC-9	HBPY-9	OPY-9	EP-9
1.607,	11.146,	10.742,	2.368,	4.456,
1.531,	2.568,	7.839,	9.260,	14.957,
17.497,	22.261,	37.099		

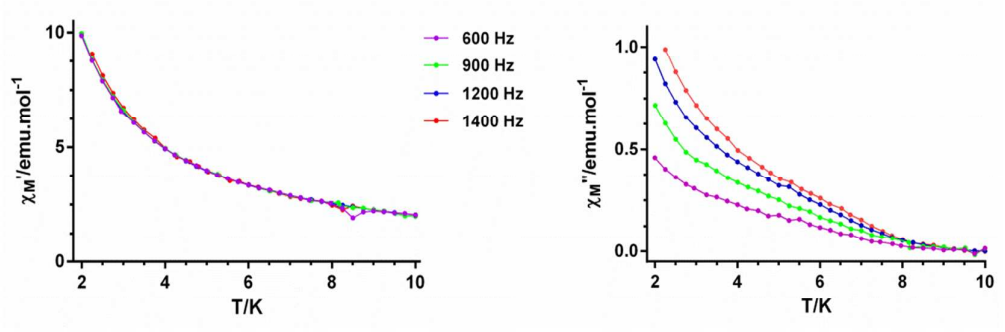

Figure S1.- Temperature dependence of in-phase χ'_M (left) and out-of-phase χ''_M (right) components of the *ac* susceptibility for complex 8 measured under zero applied *dc* field.

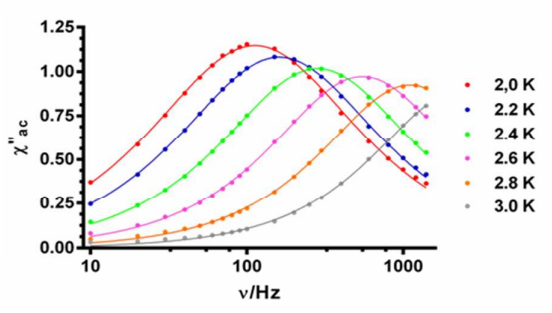

T / K	τ / s
2.4 K	0.0002653
2.6 K	0.0001768
2.8 K	0.0001326
2.9 K	0.0001137

T / K	τ / s
3.0 K	0.0000693
2.8 K	0.0001465
2.6 K	0.0002907
2.4 K	0.0005619
2.2 K	0.0009888

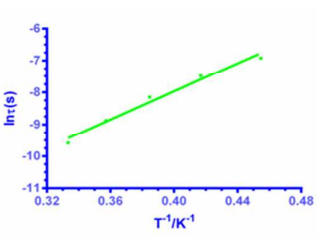

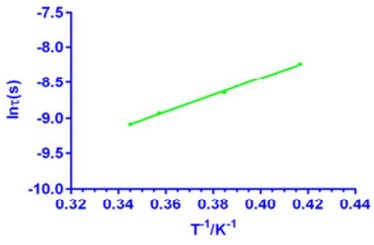

Figure S2.- Variable-temperature frequency dependence of the χ_M" signal for **5** in a 1000 Oe *dc* field. Solid lines represent the best fit to the Debye model (left top). Arrhenius plots for **5** (left down) and for **3** (right, down).

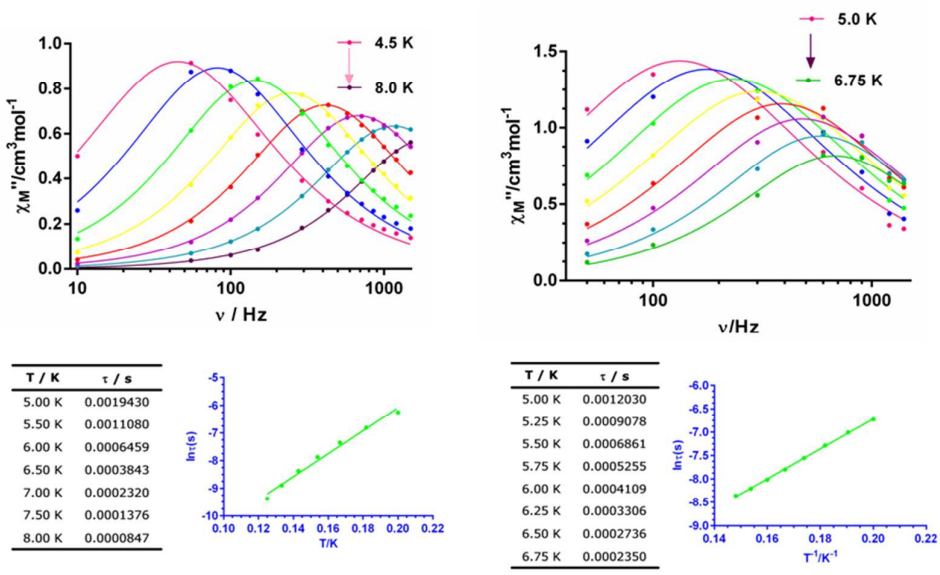

Figure S3.- Variable-temperature frequency dependence of the χ_M" signal for **2** (left top) and **8** (right top) in a 1000 Oe *dc* field. Solid lines represent the best fit to the Debye model. Arrhenius plots for **2** (left down) and for **8** (right down).

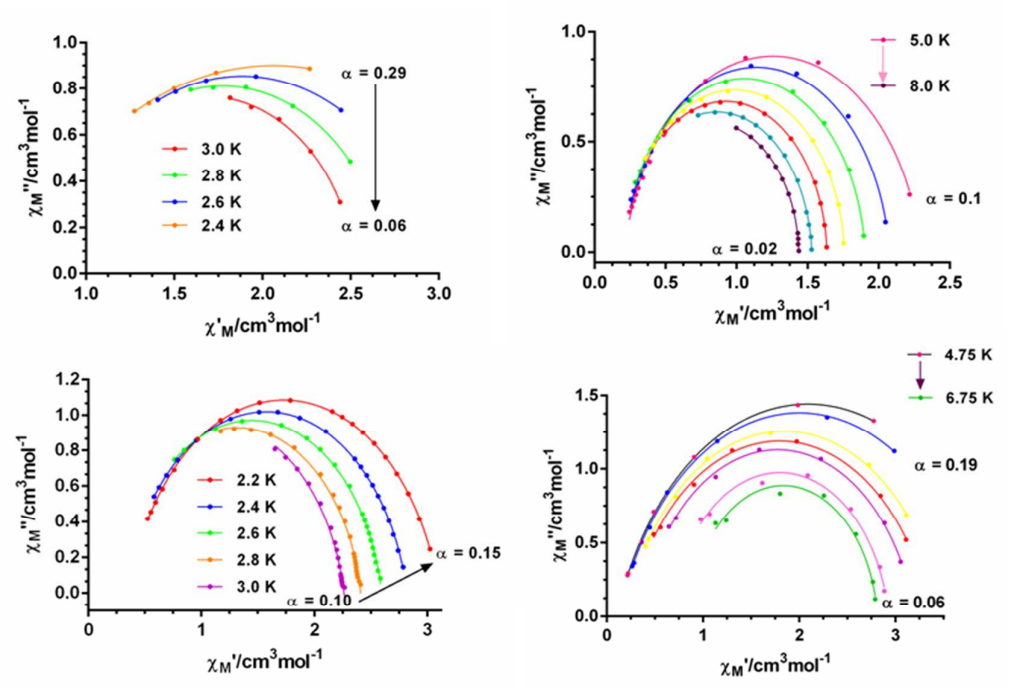

Figure S4.- Cole-Cole plots for **3** (left top), **5**(left down), **2** (right top) and **8** (right down)

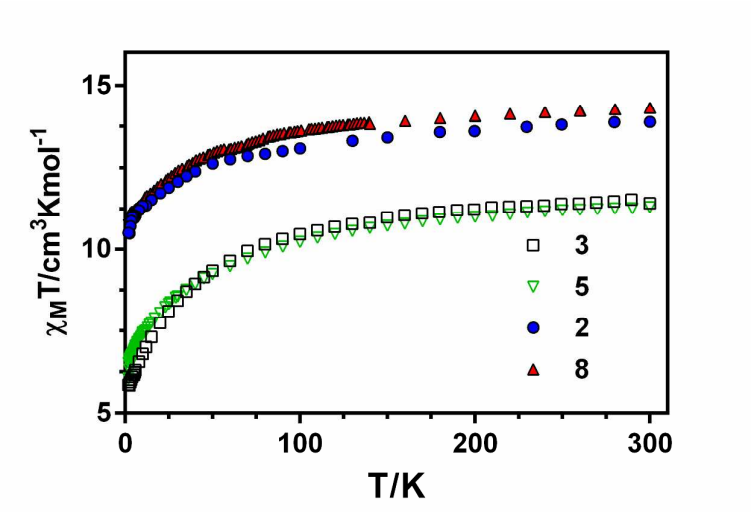

Figure S8.- Temperature dependence of the $\chi_M T$ product for complexes **2**, **3**, **5** and **8**.

The room temperature $\chi_M T$ values of Dy^{III} complexes **2** and **8** are 13.88 cm^3 $mol^{-1}K$ and 14.32 cm^3 $mol^{-1}K$, respectively, which are in rather good agreement with the expected

theoretical value using the free ion approximation (14.17 $cm^3mol^{-1}K$) for one isolated Dy^{III} ion, ($^6H_{15/2}$, S = 5/2, L = 5, g = 4/3). The χT product for **2** and **8** steadily decreases with decreasing temperature to reach minimum values of 10.50 $cm^3mol^{-1}K$ and 11.04 $cm^3mol^{-1}K$, respectively, at 2 K. The room temperature $\chi_M T$ values of Er^{III} complexes **3** and **5** are 11.41 cm^3 $mol^{-1}K$ and 11.29 cm^3 $mol^{-1}K$, respectively, which are close to the expected theoretical value using the free ion approximation (11.48 $cm^3mol^{-1}K$) for one isolated Er^{III} ion, ($^4I_{15/2}$, S = 3/2, L = 6, g = 6/5). The χT product for **2** and **8** steadily decreases with decreasing temperature to reach minimum values of 5.86 $cm^3mol^{-1}K$ and 6.04 $cm^3mol^{-1}K$, respectively, at 2 K. The decrease observed for these complexes is due to the effects of the thermal depopulation of the m_J sublevels of the ground multiplet of the Dy^{III} and Er^{III} ions, which are originated by the crystal field.

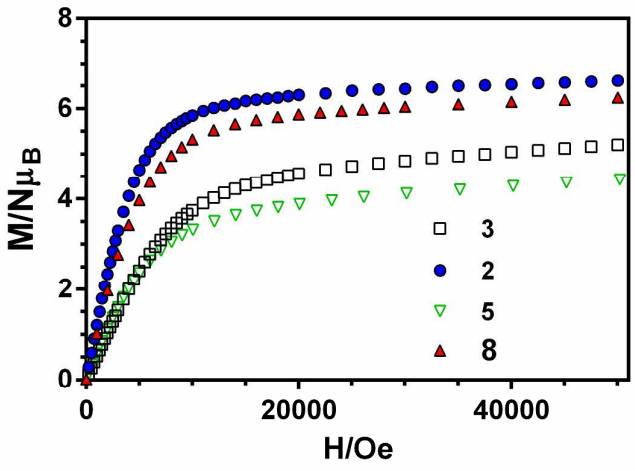

Figure S6.- Field dependence of the Magnetization for compounds **2**, **3**, **5** and **8**

The magnetization value per Dy^{III} ion at 5 T for compounds **2** and **8** and per Er^{III} ion for **3** and **5** is considerably smaller than the expected saturation value for one free Dy^{III} ion of 10 $N\square_B$ ($Ms/N\square_B = g_jJ$ = 10 $N\square_B$) and one free Er^{III} ion of ($Ms/N\square_B = g_jJ$ = 9 $N\square_B$) and is similar to those estimated and observed for other Dy^{III} and Er^{III} mononuclear complexes with approximate axial symmetry. This behavior is likely due to crystal-field effects leading to

significant magnetic anisotropy, which eliminates the 16-fold degeneracy of the $^{6}H_{15/2}$ and $^{4}I_{15/2}$ ground states, for Dy^{III} and Er^{III}, respectively

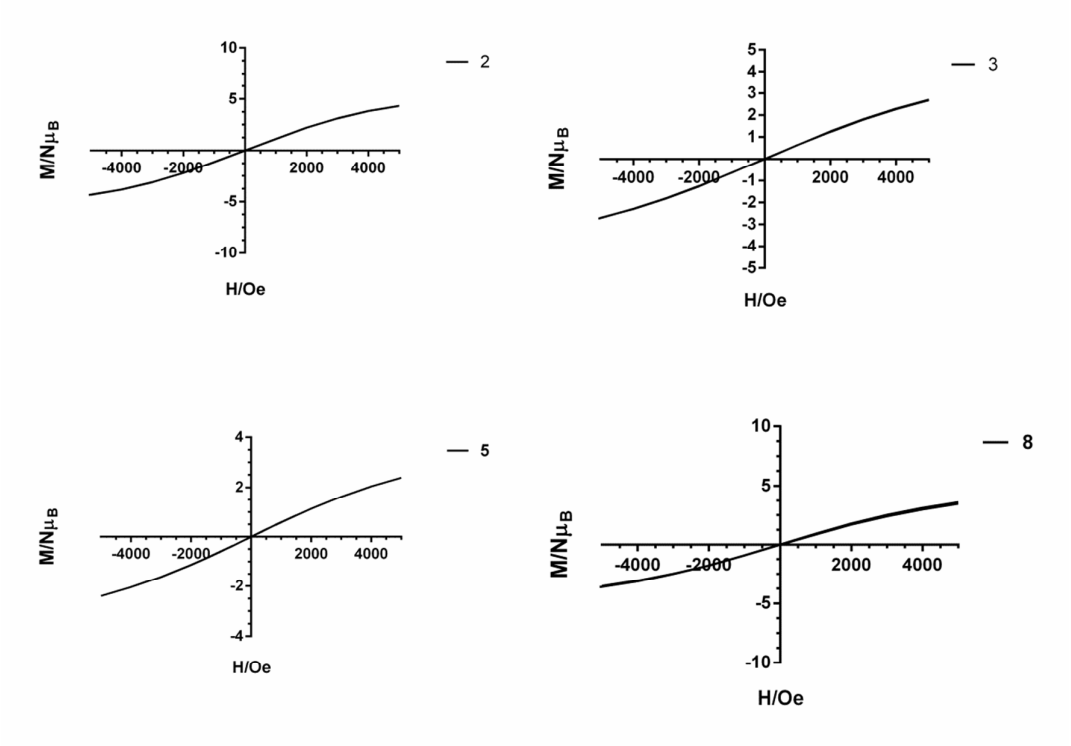

Figure S7.- Hysteresis loops for complexes **2**, **3**, **5** and **8**.

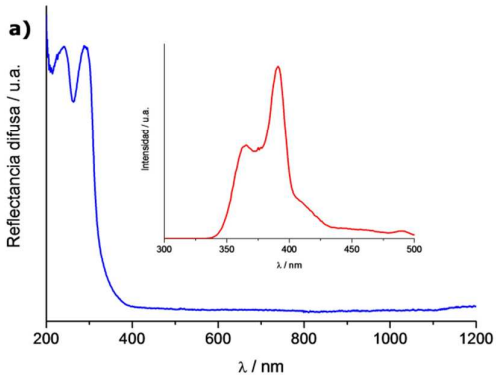

Figure S8.- Reflectance spectrum of the ligand. Emission spectrum of the ligand (inset).

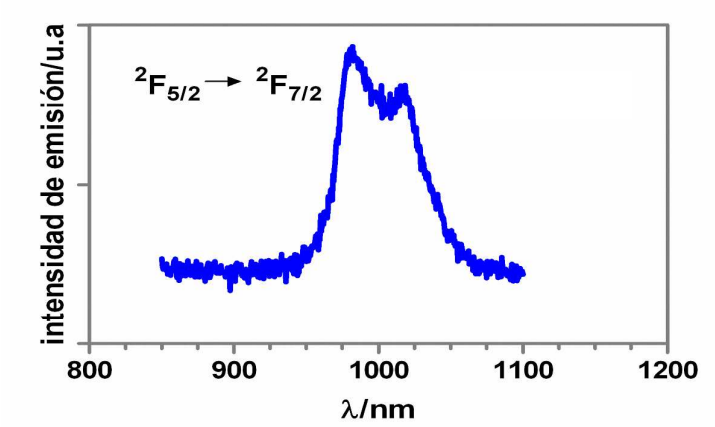

Figure S9.- NIR sensitized emission spectra of complex **4**.